Mitochondrial reactive oxygen species are scavenged by Cockayne syndrome B protein in human fibroblasts without nuclear DNA damage

James E. Cleaver[a,1], Angela M. Brennan-Minnella[b], Raymond A. Swanson[b], Ka-wing Fong[c], Junjie Chen[c], Kai-ming Chou[d], Yih-wen Chen[d], Ingrid Revet[a,e], and Vladimir Bezrookove[f]

[a]Department of Dermatology, University of California, San Francisco, CA 94143; [b]Department of Neurology, University of California, San Francisco and Veterans Affairs Medical Center, San Francisco, CA 94121; [c]Department of Experimental Radiation Oncology, University of Texas MD Anderson Cancer Center, Houston, TX 77030; [d]Department of Pharmacology and Toxicology, Indiana University School of Medicine, Indianapolis, IN 46202; [e]Department of Clinical Chemistry and Hematology, Sint Franciscus Gasthuis, 3045PM, Rotterdam, The Netherlands; and [f]Center for Melanoma Research and Treatment, California Pacific Medical Center Research Institute, San Francisco, CA 94107

Contributed by James E. Cleaver, July 25, 2014 (sent for review May 28, 2014)

Cockayne syndrome (CS) is a human DNA repair-deficient disease that involves transcription coupled repair (TCR), in which three gene products, Cockayne syndrome A (CSA), Cockayne syndrome B (CSB), and ultraviolet stimulated scaffold protein A (UVSSA) cooperate in relieving RNA polymerase II arrest at damaged sites to permit repair of the template strand. Mutation of any of these three genes results in cells with increased sensitivity to UV light and defective TCR. Mutations in CSA or CSB are associated with severe neurological disease but mutations in UVSSA are for the most part only associated with increased photosensitivity. This difference raises questions about the relevance of TCR to neurological disease in CS. We find that CSB-mutated cells, but not UVSSA-deficient cells, have increased levels of intramitochondrial reactive oxygen species (ROS), especially when mitochondrial complex I is inhibited by rotenone. Increased ROS would result in oxidative damage to mitochondrial proteins, lipids, and DNA. CSB appears to behave as an electron scavenger in the mitochondria whose absence leads to increased oxidative stress. Mitochondrial ROS, however, did not cause detectable nuclear DNA damage even when base excision repair was blocked by an inhibitor of polyADP ribose polymerase. Neurodegeneration in Cockayne syndrome may therefore be associated with ROS-induced damage in the mitochondria, independent of nuclear TCR. An implication of our present results is that mitochondrial dysfunction involving ROS has a major impact on CS-B pathology, whereas nuclear TCR may have a minimal role.

γH2Ax | oxidative DNA damage | comet assay | hydrogen peroxide | bromate

Oxidative reactions play many fundamental roles in cellular signaling, but also subject cellular components to potential damage (1–3). Consequently, cells contain numerous antioxidant compounds, detoxifying enzymes, and DNA repair enzymes that act on oxidized bases as their substrates (4). Numerous interpretations of spontaneous carcinogenesis and neurodegeneration assume that mitochondria can be a source of endogenously generated reactive oxygen species (ROS) that damage many cellular components including nuclear DNA (2, 4–8) (9–12). Whereas there seems no doubt that ROS can be generated within mitochondria (3, 13), what has not been clearly established is whether these ROS damage nuclear DNA.

This assumption of a mitochondrial origin for ROS that cause damage to nuclear DNA is central to many interpretations of the developmental and neurodegenerative phenotypes of human DNA repair-deficient diseases such as Cockayne syndrome (CS) (14–17). CS is deficient in transcription coupled repair (TCR), in which three gene products, Cockayne syndrome A (CSA), Cockayne syndrome B (CSB), and ultraviolet stimulated scaffold protein A (UVSSA) cooperate in relieving RNA polymerase II arrest at damaged sites to permit repair of the template strand (18). Most mutations in *CSA* or *CSB* are associated with severe developmental and neurological disease (19); mutations in *UVSSA* (20–22) in patients with the UV sensitive syndrome (UV^S) are associated with increased photosensitivity but mild or negligible neurological disease (23). Because mutations in either *CSA*, *CSB*, or *UVSSA* cause similar increases in UV sensitivity in vitro and cause deficiencies in TCR, the relevance of nuclear TCR of DNA damage to the clinical symptoms has become questionable.

We therefore have examined the consequences of deliberately increasing endogenous ROS production by mitochondria in normal, CS group B (CS-B) and UVSSA-deficient fibroblasts. This mode of exposure was a direct test of whether increased mitochondrial ROS can cause nuclear DNA damage that would require TCR, and the potential roles of CSB and UVSSA. We also used extracellular hydrogen peroxide as a proxy for the more stable diffusible end product of superoxide generated in many mitochondrial and cellular reactions (3, 13).

We found that CS-B mutant fibroblasts, but not UVSSA-deficient fibroblasts, have an elevated intrinsic level of mitochondrial ROS that subjects these cells to chronic oxidative stress as reported previously (24). This increased ROS, and that generated by the mitochondrial poison rotenone, a complex I inhibitor, do not however cause any detectable nuclear DNA damage. Explanations of neurodegeneration in CS should therefore consider mitochondrial dysfunction, rather than nuclear TCR, as a major cause of this disease.

Significance

Mitochondria are often considered a source of reactive oxygen species (ROS) that cause damage to cellular components including nuclear DNA. This endogenous damage is thought to underlie neurodegeneration, especially in diseases such as Cockayne syndrome (CS) that lack transcription-coupled DNA repair (TCR). We find no evidence, however, for any nuclear DNA damage from increased mitochondrial ROS. Our results indicate that the neurodegenerative symptoms in CS may be mitochondrial in origin, independent of nuclear DNA damage and repair.

Author contributions: J.E.C., A.M.B.-M., R.A.S., K.-m.C., and V.B. designed research; J.E.C., A.M.B.-M., R.A.S., K.-w.F., K.-m.C., Y.-w.C., I.R., and V.B. performed research; J.E.C., K.-w.F., J.C., and I.R. contributed new reagents/analytic tools; J.E.C., A.M.B.-M., R.A.S., K.-m.C., Y.-w.C., I.R., and V.B. analyzed data; and J.E.C., A.M.B.-M., R.A.S., K.-w.F., J.C., K.-m.C., I.R., and V.B. wrote the paper.

The authors declare no conflict of interest.

[1]To whom correspondence should be addressed. Email: JCleaver@cc.ucsf.edu.

This article contains supporting information online at www.pnas.org/lookup/suppl/doi:10.1073/pnas.1414135111/-/DCSupplemental.

Results

Two sets of isogenic fibroblasts were used for these experiments. Mutant CS-B cells [General Medical (GM)10903; Coriell Institute for Medical Research] were corrected with the normal *CSB* cDNA (called CS-B and CSB corrected in the following text). UVSSA-deficient cells were created from telomerase positive normal fibroblasts (GM05659T) with two shRNA constructs previously shown to down-regulate *UVSSA* gene expression (25). Suppression of *UVSSA* expression was monitored by Western blot and RT-PCR (Fig. S1). Unlike previous studies using HeLa cells where high levels of UVSSA expression were detected in Western blots (25), primary fibroblasts had undetectable levels of protein, but suppression of expression could be demonstrated by RT-PCR (Fig. S1). We also used two other primary CS-B fibroblasts (GM1736 and GM1428) and a telomerase-positive CS-B fibroblast (GM1428T).

Using the oxidation of dihydroethidium (dHEth) to ethidium as a measure of intracellular ROS (26), we saw a striking increase of ROS in control and rotenone-treated CS-B cells in comparison with corrected cells (Fig. 1 *A* and *B*). Ethidium is trapped in cells by binding to DNA so this assay does not identify the original sites of oxidation. ROS were also greater in CS-B cells compared with corrected cells exposed to hydrogen peroxide (Fig. 1*B*). Rotenone exposure caused additional increases in ethidium fluorescence (Fig. 1*B*). In contrast UVSSA-deficient cells showed significant reductions in oxidation, compared with controls in rotenone-treated and untreated cells. Each cell type showed a decrease in ROS with doses of rotenone higher than 1 μmol (Fig. 1 *C* and *D*). Because the UVSSA-deficient cells and isogenic controls were telomerase positive, their basal levels of ROS may not be directly comparable to those in the primary CS-B and corrected fibroblasts. Hydrogen peroxide seemed to have no effect at the dose used, although its effect on ROS levels is complex because it does not directly oxidize dihydroethidium (or Mitosox) in simple aqueous solution. The induction of ROS in CS-B and corrected fibroblasts after exposure to hydrogen peroxide or rotenone was also determined using Mitosox, which demonstrated a predominantly cytoplasmic fluorescence (Fig. S2).

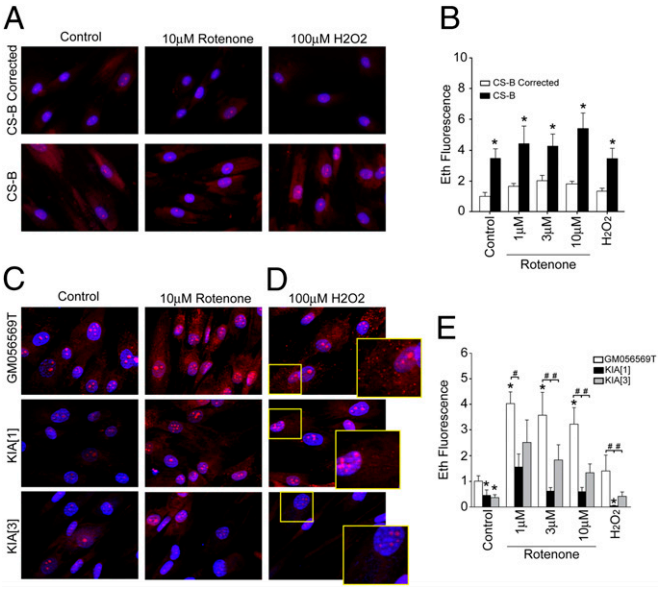

Fig. 1. dHEth oxidation in CS-B, UVSSA-deficient, and isogenic normal cells exposed to rotenone or hydrogen peroxide. (*A* and *B*) Ethidium fluorescence in CS-B and corrected cells. (*C–E*) dHEth oxidation in normal, GM05659T, cells and KIA[1] and KIA[3] cells with *UVSSA* suppressed. *D* shows enlarged panels to show distribution of Eth; scale of *y* axis in *B* and *E* is normalized to the respective normal control set to 1.0. Error bars represent SDs for $n = 3$.

Cell survival is commonly assayed colorimetrically by the reduction of 3-(4,5-dimethylthiazol-2-yl)-2,5-diphenyltetrazolium bromide (MTT) to formazon, resulting in a purple dye measured by absorbance at 570 nm. Because rotenone exposure caused changes in redox balance of the cells (Fig. 1 *A–C*), colorimetric changes seen with MTT may be influenced by cellular reductive capacity in addition to the number of viable cells. We determined the dose–response for MTT reduction in CS-B and corrected cells and UVSSA-deficient cells grown after exposure to UV light or inhibitors of mitochondrial complex I (rotenone), II (3-nitropropionic acid, 3NP), and III (antimycin) (Fig. 2 *A–D* and Fig. S3 *A–C*). After UV exposure, which damages DNA directly with minimal changes in ROS, MTT demonstrated increased sensitivity characteristic of the reduced TCR of CS-B and cells with reduced UVSSA expression (Fig. 2 *A* and *B*). The increase in UV sensitivity of UVSSA-deficient cells is similar to that observed in HeLa cells with these shRNA vectors (25) despite differences in basal levels of UVSSA protein (Fig. S1). The UVSSA-deficient cells were not as sensitive to UV light as CS-B, due to the persistence of reduced levels of UVSSA (Fig. S1) compared with CS-B, which is a nonfunctional truncation mutation. Rotenone-treated CS-B cells compared with corrected cells, however, showed a dramatic inversion of the response seen with UV light (Fig. 2*C*). Rotenone's impact was suppressed by a ROS quencher, tetramethylisoindolin-2-yloxyl (CTMIO) (Fig. S3) (27). The robust reduction of MTT to its purple product in the presence of rotenone was consistent when tested in three unrelated CS-B cell lines (Fig. S4*A*). CS-B cells maintained a high level of MTT reduction compared with corrected cells, indicating an increased release of electrons from oxidative phosphorylation into the mitochondrial matrix. UVSSA-deficient cells, however, showed the same reduction in MTT absorbance as normal cells when exposed to rotenone (Fig. 2*D* and Fig. S4*A*). Neither 3NP (Fig. S4*B*) nor antimycin (Fig. S4*C*) showed any difference between CS-B and corrected cells. These observations show that CS-B cells have a unique response involving elevated ROS from dysregulation of mitochondrial complex I.

Cell survival determined by counting cell numbers at 7 d following the start of exposure showed no difference between CS-B and corrected cells exposed to either rotenone (Fig. 2*E*) or hydrogen peroxide (Fig. 2*F*). The increased ROS in CS-B (Fig. 1 *A* and *B*) does not therefore directly impact cell survival, but rather may have induced senescence in both cell types (28).

Single strand breaks (SSBs) in nuclear DNA from hydrogen peroxide and rotenone was determined by the alkaline comet assay (Trevigen; *SI Materials and Methods* and *SI Results*). CS-B and CS-B corrected cells were treated with or without rotenone or hydrogen peroxide for 4 h before mixing with low melting point agarose and analysis. Extensive DNA damage was evident in cells exposed to hydrogen peroxide, but none from rotenone exposure (Fig. 3*A* and Fig. S5).

γH2Ax was examined using Western blots and immunofluorescence (IF). In Western blots, γH2Ax was detected after hydrogen peroxide exposure but not after rotenone exposure (Fig. 3*B*) as reported previously using nonisogenic cells (29). Western blots represent an average over the whole population so we also examined γH2Ax by IF (Fig. 4 *A–D*). Exposure to hydrogen peroxide or UV light showed large increases in the pixel intensities and percentages of positive cells (Fig. 4 *A–D*). Hydrogen peroxide showed clustered foci of γH2Ax typical of DNA breaks (Fig. 3 *A* and *B*), consistent with results from the comet assay (Fig. 3*A*). In cells exposed to rotenone less than 10% of the population were positive for γH2Ax and there was no significant difference between CS-B and CSB-corrected cells (Fig. 4 *A–C*). In unexposed cells, a small fraction of CS-B cells showed higher intensities and percentages of positive cells than the corrected cells (Fig. 4 *A–D*), which decreased after rotenone exposure. We

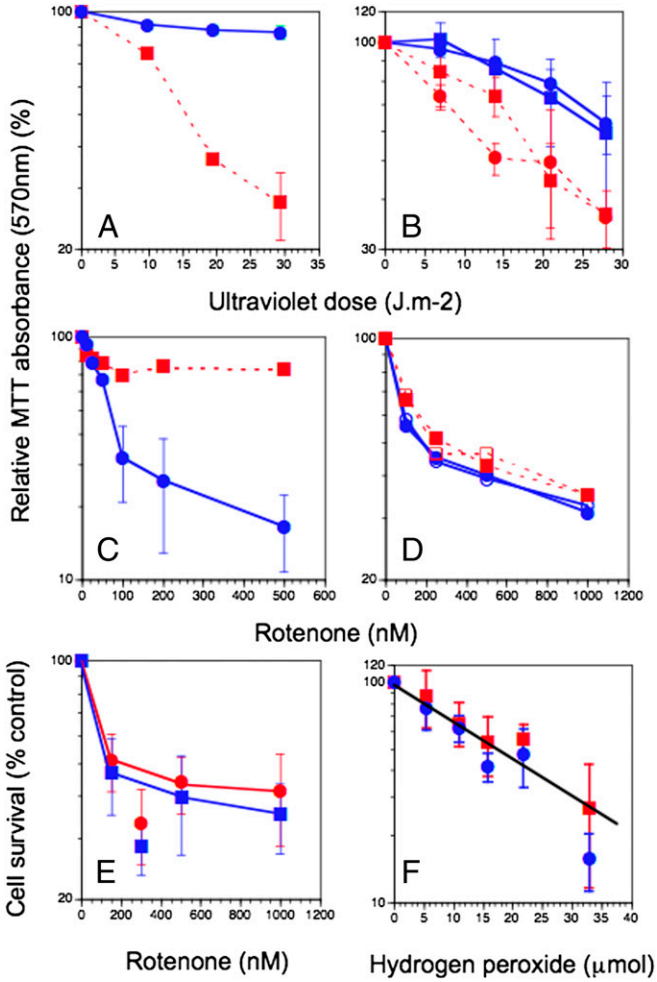

Fig. 2. Relative MTT levels in CS-B (red), UVSSA (red), and isogenic normal cells (blue) exposed to rotenone, UV light, and hydrogen peroxide. (*A*) Relative MTT levels in CS-B and corrected cells exposed to UV light. (*B*) Relative MTT levels in normal (GM05659T), KIA[1], and KIA[3] cells exposed to UV light. (*C*) Relative MTT levels in CS-B and corrected cells exposed to rotenone. (*D*) Relative MTT levels in normal (GM05659T), KIA[1] and KIA[3] cells exposed to rotenone. (*E*) Relative cell numbers in CS-B and corrected cells exposed to rotenone. (*F*) Relative cell numbers in CS-B and corrected cells exposed to hydrogen peroxide. Error bars represent SDs for $n = 3$ or more determinations; when no error bars are shown the SDs were smaller than the size of the symbols.

examined whether rotenone could have caused this decrease by a reduction in available ATP for γH2Ax formation. However, in cells exposed to both rotenone and UV, there was no reduction in γH2Ax compared with UV alone (Fig. S6).

We may have been unable to detect DNA damage due to a rapid turnover of lesions by base excision repair (BER). We therefore increased resolution of damage by inhibiting poly (ADP ribose) polymerase (PARP-1), an essential cofactor for BER (30), with the drug ABT888 (Abbott Laboratories). Normal fibroblasts (GM05659T), which showed a large increase in dHEth oxidation after exposure to rotenone (Fig. 1*D*), showed no increase in cell death assayed either by MTT or cell numbers (Fig. 5 *A* and *B*) when grown in ABT888. CS-B (GM1428T) and normal (GM05659T) cells showed identical response to the toxic effect of increasing levels of ABT888, implying there was no DNA damage involving BER present in these cells under ambient conditions (Fig. 5*C*).

In contrast, in cells damaged by temozolomide, a chemotherapeutic alkylating agent that causes damage that requires BER, growth in ABT888 resulted in increased cell killing (Fig. 5*D*), although there was no difference in sensitivity between CS-B and normal cells (Fig. S7*A*). CS-B cells were more sensitive than normal cells to potassium bromate that makes 8-oxo-dG in DNA (31) (37% surviving dose 0.4 versus 0.57 mM) and both showed increased sensitivity when grown in ABT888 (37% surviving dose 0.07 versus 0.41 mM). We did not detect any effect of ABT888 on normal (GM05659T) cells grown in hydrogen peroxide (Fig. S7*B*). ABT888 also had no impact on γH2Ax in control or rotenone exposed CS-B, CS-B corrected, or GM05659T cells (Fig. S8).

Discussion

This work has proceeded on two major themes: (*i*) Could we verify a common assumption that byproducts from oxidative phosphorylation in the mitochondria cause nuclear DNA damage (2, 4–8) (9–11) and (*ii*) What roles do CSB and UVSSA play in cellular redox balance? Our conclusions impact our understanding of the endogenous causes of neurodegeneration in repair-deficient disease.

This work was based on the toxicity of rotenone that interferes with electron transfer from Fe-S clusters in mitochondrial complex I to ubiquinone. Rotenone reduces NADH and ATP production and diverts electrons into the mitochondrial matrix to create ROS (2, 3). Reduced ATP eventually results in cessation of growth that can lead to senescence (28). Increased mitochondrial ROS could damage proteins, lipids, and DNA within the mitochondria. Superoxide, one of the inital ROS products, is an anion and rarely passes through cell membranes. Nonpolar superoxide metabolites such as hydrogen peroxide do pass out of the mitochondria into the cytoplasm and cause oxidative damage. Our results in CS-B and UV^s cells indicate that ATP starvation and ROS production may have separable consequences. The loss of CSB increased mitochondrial ROS (Fig. 1 *A–D*) and increased MTT reduction (Fig. 2*C*), but cessation of growth

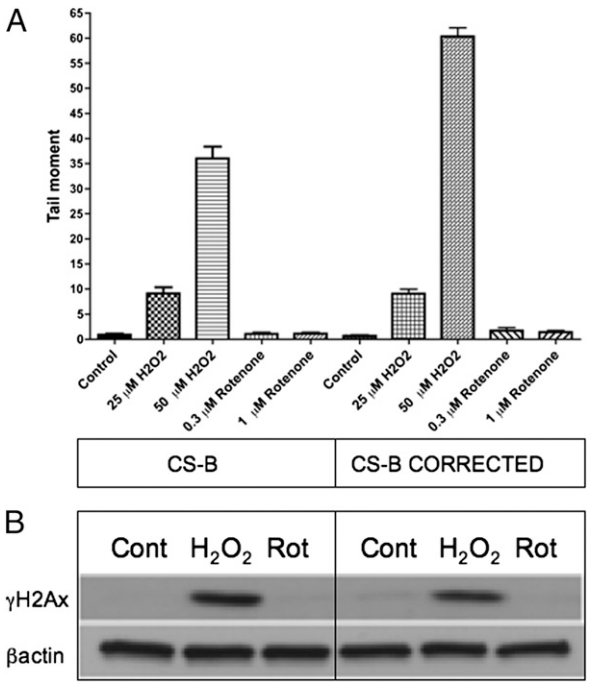

Fig. 3. DNA single strand breaks and double strand breaks. (*A*) Single strand breaks determined by Comet assay in CS-B and isogenic corrected CS-B cells exposed to hydrogen peroxide or rotenone (for images, Fig. S5). (*B*) Western blot showing induction of γH2Ax indicative of double strand breaks in CS-B and isogenic-corrected CS-B cells exposed to hydrogen peroxide or rotenone. Error bars represent SDs for $n = 3$.

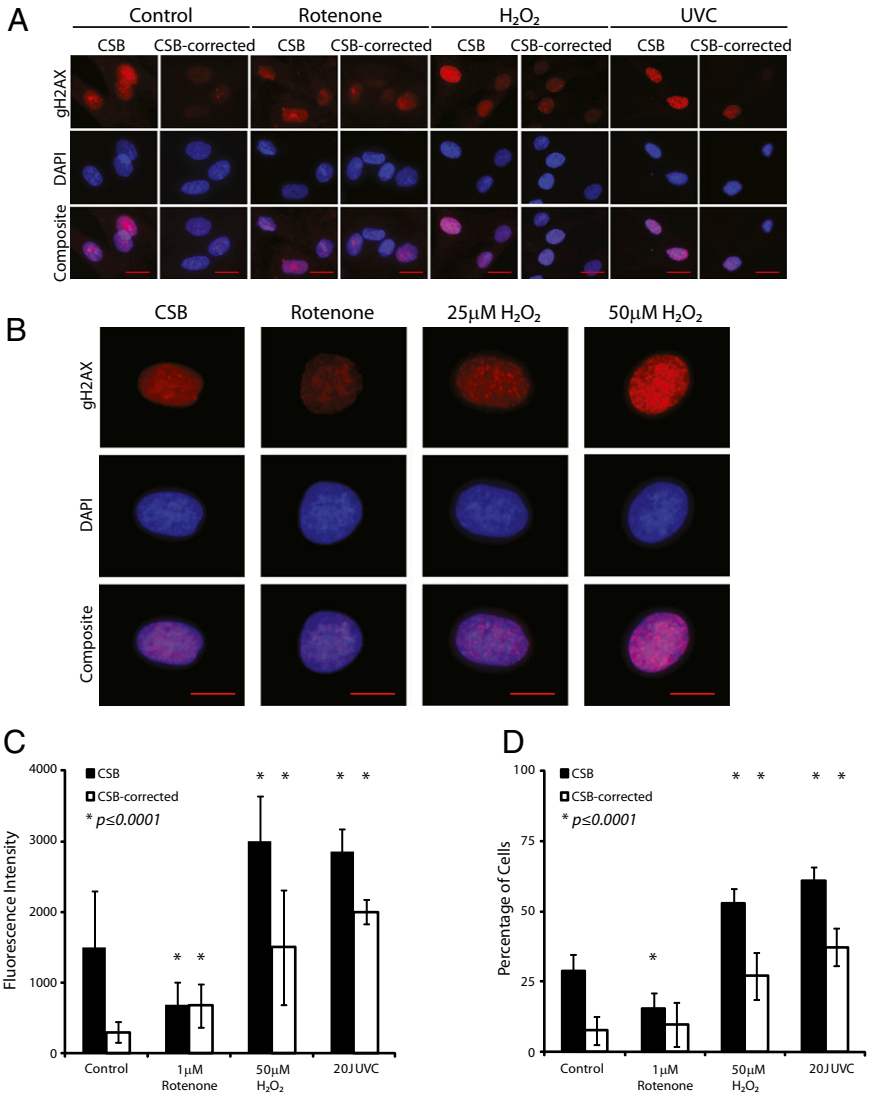

Fig. 4. Differential expression of γH2Ax in CS-B and CSB + WT cDNA cells after exposure to rotenone, hydrogen peroxide, or UV compared with nontreated cells. (*A*) IF images of γH2AX (red) in CS-B and isogenic-corrected CS-B cells. Before immunodetection, cells were cultured for 4 h in presence of rotenone (1 μM) or hydrogen peroxide (50 μM) or after UVC (20 J/m2). DAPI (blue) was used to counterstain nuclei. (Scale bar, 20 μm.) (*B*) Higher power images showing reduced IF in rotenone-exposed cells and foci after hydrogen peroxide. (*C*) Bar graph representing the mean pixel intensity of γH2AX in CS-B and CS-B–corrected cells. Error bars represent SD of measurments of two independent experiments with at least 500 nuclei per measurement. Statistical significance ($P \leq 0.0001$) of each cell type compared with its control was tested by using Mann–Whitney *u* test. (*D*) Bar graph for percentage of γH2AX-positive cells (+2σ) in CS-B and CS-B–corrected cells, calculated from fluorescence intensity measurements. Error bars represent 95% confidence interval. Statistical significance (*$P \leq 0.0001$) of each cell type compared with its control was calculated using Z test for two population proportions.

in both CS-B and corrected cells was similar, presumably due to ATP starvation (Fig. 2*E*). A redox-related degeneration of neuronal structure would likely be more important in neurons, because few are proliferating and effects on growth would be moot. The CSB protein, therefore, plays no differential role in blockage of ATP production. Instead CSB acts as an electron sink affecting mitochondrial ROS levels by interaction with complex I, but not complex II or III. This role for the CSB protein must be seen in addition to its multiple roles in nuclear chromatin maintenance, the transcription response to hypoxia, and TCR (reviewed in ref. 29).

The lower levels of ROS induced in UVSSA-deficient cells than in normal cells (Fig. 1 *C* and *D*) may be due to the presence of higher levels of mitochondrial CSB, that was not otherwise involved in nuclear TCR due to the loss of UVSSA. This difference between ROS levels was not sufficient to be resolved in the MTT assay (Fig. 2*D*). Whether CSA plays a similar role to CSB in regulating ROS remains to be determined, but one report suggests that CSA does play a role in repair of oxidative damage (32).

Our results imply that the CSB protein's mitochondrial function as an electron sink is closely allied to complex I. This function might be similar to that of the Parkinson disease protein Pink1 that is also linked to electron transport deficiencies in complex I (33). The higher levels of mitochondrial ROS in CS-B cells may underlie the morphological abnormalities and increased autophagy seen in Cs-b mice (29, 34, 35), although Cs-b mice show very mild symptoms unless crossed with other repair-deficient strains (35, 36). Despite major changes in mitochondrial ROS levels and the cellular redox balance (24), we found no evidence for detectable nuclear DNA damage, based on breakage and γH2Ax assays (Figs. 3 and 4 and Fig. S5). Increased cell killing by inhibition of the PARP-1 component of BER was detectable in cells damaged by an alkylating or oxidizing agent but not after

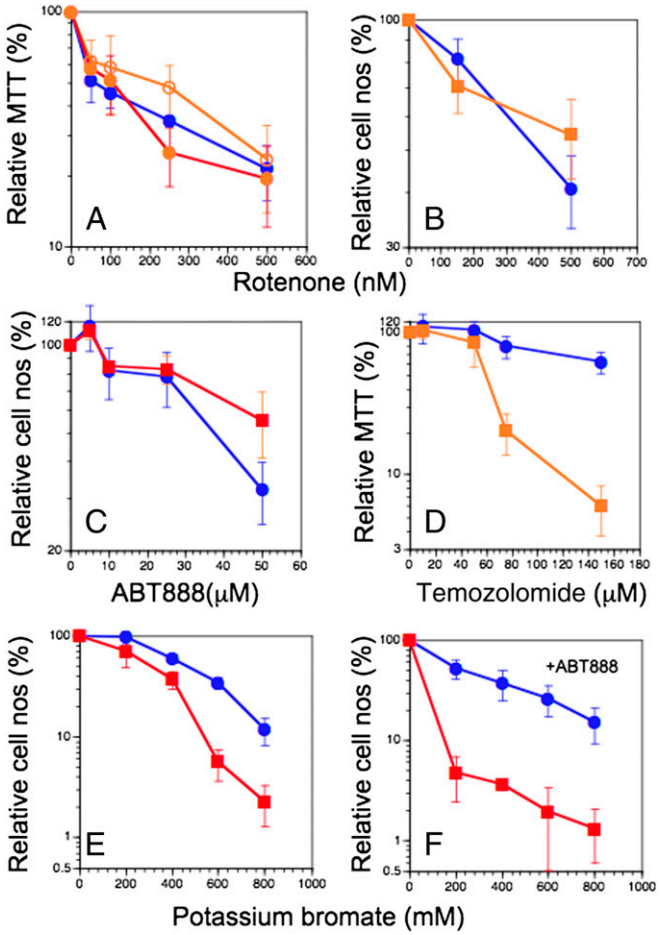

Fig. 5. Sensitivity of GM05659T or GM01428 cells grown for 7 d after exposure (open orange circles, 10 μM; closed orange circles, 25 μM; without ABT888TM, blue; GM1428, red). (*A*) Relative MTT levels exposed to rotenone with or without PARP inhibition. (*B*) Relative cell numbers in cells exposed to rotenone with or without 25 μM ABT888TM. (*C*) Relative cell numbers in cells exposed to a range of concentrations of the PARP-1 inhibitor ABT888 TM. (*D*) Relative MTT levels in cells exposed to temozolomide with or without 25 μM ABT888TM. (*E*) GM05659T and GM01428T cells exposed to potassium bromate and grown in medium only. (*F*) GM05659T and GM01428T cells exposed to potassium bromate and grown in medium plus ABT888TM 25 μM. Error bars represent SDs for $n = 3$ or more determinations; when no error bars are shown the SDs were smaller than the size of the symbols.

rotenone exposure. Thus, inhibiting PARP-1 did not reveal any oxidative DNA damage from exposure to rotenone.

The minor histone H2Ax is phosphorylated by the ataxia telangiectasia mutated kinase that is an oxygen sensor (37). In the presence of DNA double stranded breaks (DSBs), γH2Ax forms clustered nuclear foci but under other stresses such as UV forms diffuse distributions (38–40). We observed high levels of γH2Ax in CS-B cells, greater than corrected cells, after hydrogen peroxide and UV light but similar low levels in cells exposed to rotenone (Fig. 4 *C* and *D*). In GM05659T cells, rotenone exposure increased the level of γH2Ax to a small extent, but because these are more rapidly growing telomerase-positive cells, this may represent a cell-cycle–dependent response not associated with DNA breakage. In control CS-B cells, the level of γH2Ax was slightly higher than CS-B corrected (Fig. 4), which may represent a cellular stress response, but this was not associated with any evidence for DNA breakage by the comet assay (Fig. 3*A*). Nuclear base damage from ROS requires BER that involves PARP-1 as an essential cofactor. However, we found no increase in toxicity in cells exposed to rotenone when BER was inhibited by ABT888, although increases were observed in cells exposed to temozolomide and potassium bromate (Fig. 5 *A*–*F*). Mitochondrial oxidation was also not a source of nuclear 8-oxo-dG in HeLa cells (41).

The response of cells to hydrogen peroxide deserves special mention. This oxidizing agent is the more stable, diffusible product generated from superoxide in mitochondria (13). CS-B cells were not however more sensitive than normal cells (Fig. 2*F*), and cell killing from hydrogen peroxide was not sensitized by ABT888 (Fig. S7*B*). We conclude that hydrogen peroxide under the conditions used here (37 °C in medium) mainly generates DNA breaks, but insignificant levels of those kinds of base damage to which CS-B cells may be more sensitive (16). One inference from these observations is that inflammatory and oxidase reactions that produce hydrogen peroxide in vivo are unlikely to be sources of CS-B pathology, unless like X-rays, they also produce minor base damage that requires TCR (42).

Our results show that there is no intrinsic oxidative damage to nuclear DNA from mitochondrial sources in human fibroblasts in vitro, even when mitochondrial ROS is elevated due to rotenone or inactivating mutation of *CSB*. In vivo, however, there are many extrinsic sources of ROS that may contribute to oxidative damage, especially in neural tissue, as recently demonstrated with the glutamate analog *N*-methyl-D-aspartate (NMDA) (26). Extrinsic sources of ROS may contribute to the increased levels of oxidative damage to nuclear DNA reported in Cs-b mice (43).

In contrast to the mitochondrial function of CSB that differs markedly from that of UVSSA, these two proteins play coordinating roles in the nuclear TCR pathway and in cellular sensitivity to UV light (Fig. 2 *A* and *B*). Patients with CS-B, however, have very severe clinical symptoms of development and neurodegeneration, whereas patients with UV^s with mutations in *UVSSA* mainly exhibit photosensitivity. An implication of our present results is that mitochondrial dysfunction involving ROS may have a major impact on CS-B pathology, whereas nuclear TCR has a minimal role, unless neuronal cells in vivo are exposed to extracellular sources of ROS that damage nuclear DNA.

Materials and Methods

Primary fibroblasts (CS-B: GM10903, GM01736, and GM01428; and normal: GM05659) were obtained from the Coriell Cell Repositories. GM05659T and GM01428T were derived inhouse by lentivirus infection with hTERT and selected in blastocidin. The CS-B cell line is homozygous for the c2282t, Arg735stop mutation, which produces cells with no full-length CSB protein. Cells were grown in Eagle's MEM, supplemented with 10% (vol/vol) FCS, L-glutamine, and 10 units penicillin, 10 μg/mL streptomycin. All cells were maintained at 37 °C, in a humidified atmosphere containing 5% (vol/vol) CO_2.

The CS-B cell line was corrected with wild-type *CSB* cDNA. pFB-Neo (Stratagene) and pFastBac CSB (44) were provided by Pablo Rodriguez (University of California, San Francisco) and Cliff Ng (Lawrence Berkeley National Laboratory, Berkeley, CA), respectively. The *CSB* cDNA with a NH2-terminal HA-tag derived from pFastBac *CSB* was cloned into the pFB-Neo retroviral vector. The resulting constructs were packaged in Phoenix-Ampho cells (Stanford University, Stanford, CA) by transfection with Fugene 6 (Roche) according to the manufacturer's instructions. Supernatant fluids from individual Phoenix-Ampho cells were used to infect GM10903 primary fibroblast at a 1:2 dilution in MEM media. Cells were passaged after 4 d and selected with 300 μg/mL G418 for 14 d.

Suppression of *UVSSA* expression in GM05659T cells was achieved using shRNAs described in detail previously (25). Lentivirus containing the shRNA sequences linked to GFP and the selection marker for puromycin resistance were used to infect a normal human fibroblast GM05659T that had been previously immortalized with human telomerase hTERT. An empty lentivirus had no impact on the UV response and so was not used extensively. Expression of shRNAs was confirmed by puromycin resistance, GFP fluorescence, RT-PCR (Fig. S1), and increased sensitivity to UV light (Fig. 2). Protein expression in the parent GM05659T cell line was insufficient for Westerns to be informative (Fig. S1).

The levels of superoxide were determined using the dyes dihydroethidium (dHEth, 5 μM; Life Technologies) and Mitosox (5 μM; Life Technologies) that were loaded into cells for 10–20 min before exposures and maintained throughout the assay (*SI Materials and Methods* and *SI Results*).

Cells were exposed to ultraviolet light C (UVC; 254 nm at a fluency of 1.4 $J \cdot m^{-2} \cdot s$) in multiwell plates for cell survival or 100-mm dishes for protein extraction and Western blots. Cells were also exposed to a range of concentrations of rotenone, hydrogen peroxide, temozolomide, and potassium bromate (Sigma-Aldrich) or the PARP-1 inhibitor ABT888 (Abbott Laboratories) continuously in normal growth medium. After the start of exposure, cells were allowed to grow for 5–7 d and survival was measured by either counting the cell number or by measuring colorimetric activation of MTT (Sigma-Aldrich). Relative survival was calculated from the ratios of exposed to unexposed wells based on the average of four to six wells per exposure condition.

SSBs in nuclear DNA were determined by alkaline comet assay (*SI Materials and Methods* and *SI Results*) using the assay kit following the manufacturer's instructions (Trevigen). DNA damage was calculated as percent DNA in the tail using TriTek Cometscore 1.5 software. The study was repeated independently three times and Student *t* test was performed using Prism 4 (GraphPad software).Western blots and immunohistochemistry were carried out to determine expression of γH2Ax and pCHK2, as described previously (*SI Materials and Methods* and *SI Results*) (40). γH2Ax(ser139) antibody was obtained from Cell Signaling and β-actin antibody from Upstate Laboratories. Detection and quantification of γH2Ax using immunofluorescence was performed on cells cultured on coverslips as described (45). The anti-γH2Ax (1:1,000 dilution) was detected with secondary antibodies labeled with Alexa Fluor 594, respectively (both at 1:1,000 dilution; Molecular Probes). Images were taken at fixed exposures with a Zeiss Axio Image Z2 microscope, and the fluorescence intensities of individual cells were quantified by using ImageJ software. The mean pixel intensities were used for statistical analysis using Microsoft Excel and Data Desk.

ACKNOWLEDGMENTS. We thank Dr. S. Bottle (School of Physical and Chemical Sciences, Queensland University of Technology) for the gift of CTMIO and Gary Green, Luzviminda Feeney, and Staci Hoell for technical assistance. This work was initiated by support from the National Institute of Neurological Disease and Stroke 1R01052781 (to J.E.C.) and the Luke O'Brien Foundation (J.E.C.) and subsequent support was from the E. A. Dickson Emeritus Professorship of the University of California, San Francisco (UCSF) (J.E.C.) and the Simon Memorial Fund of the UCSF Academic Senate Memorial Fund (J.E.C.). Additional support came from National Institutes of Health Grants NS 041421 (to R.A.S. and A.M.B.-M.), CA 092312 (to J.E.C. and K.-w.F.), CA 112446 (to K.-m.C.), and the Department of Veterans Affairs (R.A.S. and A.M.B.-M.).

1. Lindahl T (1993) Instability and decay of the primary structure of DNA. *Nature* 362(6422):709–715.
2. Wallace DC (2005) A mitochondrial paradigm of metabolic and degenerative diseases, aging, and cancer: A dawn for evolutionary medicine. *Annu Rev Genet* 39:359–407.
3. Halliwell B, Gutteridge JMC (2007) *Free Radicals in Biology and Medicine* (Oxford Univ Press, Oxford).
4. Barnes DE, Lindahl T (2004) Repair and genetic consequences of endogenous DNA base damage in mammalian cells. *Annu Rev Genet* 38:445–476.
5. Bindokas VP, Jordán J, Lee CC, Miller RJ (1996) Superoxide production in rat hippocampal neurons: Selective imaging with hydroethidine. *J Neurosci* 16(4):1324–1336.
6. Adam-Vizi V, Chinopoulos C (2006) Bioenergetics and the formation of mitochondrial reactive oxygen species. *Trends Pharmacol Sci* 27(12):639–645.
7. Barzilai A, Rotman G, Shiloh Y (2002) ATM deficiency and oxidative stress: A new dimension of defective response to DNA damage. *DNA Repair (Amst)* 1(1):3–25.
8. Hoeijmakers JH (2001) Genome maintenance mechanisms for preventing cancer. *Nature* 411(6835):366–374.
9. Geyfman M, et al. (2012) Brain and muscle Arnt-like protein-1 (BMAL1) controls circadian cell proliferation and susceptibility to UVB-induced DNA damage in the epidermis. *Proc Natl Acad Sci USA* 109(29):11758–11763.
10. Zhang G, et al. (2013) Comparative analysis of bat genomes provides insight into the evolution of flight and immunity. *Science* 339(6118):456–460.
11. Gut P, Verdin E (2013) The nexus of chromatin regulation and intermediary metabolism. *Nature* 502(7472):489–498.
12. Koren I, Kimchi A (2012) Cell biology. Promoting tumorigenesis by suppressing autophagy. *Science* 338(6109):889–890.
13. Adam-Vizi V, Starkov AA (2010) Calcium and mitochondrial reactive oxygen species generation: How to read the facts. *J Alzheimers Dis* 20(Suppl 2):S413–S426.
14. de Waard H, et al. (2003) Cell type-specific hypersensitivity to oxidative damage in CSB and XPA mice. *DNA Repair (Amst)* 2(1):13–25.
15. Gorgels TG, et al. (2007) Retinal degeneration and ionizing radiation hypersensitivity in a mouse model for Cockayne syndrome. *Mol Cell Biol* 27(4):1433–1441.
16. Spivak G, Hanawalt PC (2006) Host cell reactivation of plasmids containing oxidative DNA lesions is defective in Cockayne syndrome but normal in UV-sensitive syndrome fibroblasts. *DNA Repair (Amst)* 5(1):13–22.
17. Scheibye-Knudsen M, Croteau DL, Bohr VA (2013) Mitochondrial deficiency in Cockayne syndrome. *Mech Ageing Dev* 134(5-6):275–283.
18. Cleaver JE (2012) Photosensitivity syndrome brings to light a new transcription-coupled DNA repair cofactor. *Nat Genet* 44(5):477–478.
19. Cleaver JE, Lam ET, Revet I (2009) Disorders of nucleotide excision repair: The genetic and molecular basis of heterogeneity. *Nat Rev Genet* 10(11):756–768.
20. Zhang X, et al. (2012) Mutations in UVSSA cause UV-sensitive syndrome and destabilize ERCC6 in transcription-coupled DNA repair. *Nat Genet* 44(5):593–597.
21. Schwertman P, et al. (2012) UV-sensitive syndrome protein UVSSA recruits USP7 to regulate transcription-coupled repair. *Nat Genet* 44(5):598–602.
22. Nakazawa Y, et al. (2012) Mutations in UVSSA cause UV-sensitive syndrome and impair RNA polymerase IIo processing in transcription-coupled nucleotide-excision repair. *Nat Genet* 44:586–592.
23. Fujiwara Y, Ichihashi M, Kano Y, Goto K, Shimizu K (1981) A new human photosensitive subject with a defect in the recovery of DNA synthesis after ultraviolet-light irradiation. *J Invest Dermatol* 77(3):256–263.
24. Pascucci B, et al. (2012) An altered redox balance mediates the hypersensitivity of Cockayne syndrome primary fibroblasts to oxidative stress. *Aging Cell* 11(3):520–529.
25. Fei J, Chen J (2012) KIAA1530 protein is recruited by Cockayne syndrome complementation group protein A (CSA) to participate in transcription-coupled repair (TCR). *J Biol Chem* 287(42):35118–35126.
26. Brennan AM, et al. (2009) NADPH oxidase is the primary source of superoxide induced by NMDA receptor activation. *Nat Neurosci* 12(7):857–863.
27. Chen P, et al. (2003) Oxidative stress is responsible for deficient survival and dendritogenesis in purkinje neurons from ataxia-telangiectasia mutated mutant mice. *J Neurosci* 23(36):11453–11460.
28. Noppe G, et al. (2009) Rapid flow cytometric method for measuring senescence associated beta-galactosidase activity in human fibroblasts. *Cytometry A* 75(11):910–916.
29. Cleaver JE, Bezrookove V, Revet I, Huang EJ (2013) Conceptual developments in the causes of Cockayne syndrome. *Mech Ageing Dev* 134(5-6):284–290.
30. Masson M, et al. (1998) XRCC1 is specifically associated with poly(ADP-ribose) polymerase and negatively regulates its activity following DNA damage. *Mol Cell Biol* 18(6):3563–3571.
31. Kawanishi S, Murata M (2006) Mechanism of DNA damage induced by bromate differs from general types of oxidative stress. *Toxicology* 221(2–3):172–178.
32. D'Errico M, et al. (2007) The role of CSA in the response to oxidative DNA damage in human cells. *Oncogene* 26(30):4336–4343.
33. Morais VA, et al. (2014) PINK1 loss-of-function mutations affect mitochondrial complex I activity via NdufA10 ubiquinone uncoupling. *Science* 344(6180):203–207.
34. Scheibye-Knudsen M, et al. (2012) Cockayne syndrome group B protein prevents the accumulation of damaged mitochondria by promoting mitochondrial autophagy. *J Exp Med* 209(4):855–869.
35. Revet I, Feeney L, Tang AA, Huang EJ, Cleaver JE (2012) Dysmyelination not demyelination causes neurological symptoms in preweaned mice in a murine model of Cockayne syndrome. *Proc Natl Acad Sci USA* 109(12):4627–4632.
36. Laposa RR, Huang EJ, Cleaver JE (2007) Increased apoptosis, p53 up-regulation, and cerebellar neuronal degeneration in repair-deficient Cockayne syndrome mice. *Proc Natl Acad Sci USA* 104(4):1389–1394.
37. Guo Z, Kozlov S, Lavin MF, Person MD, Paull TT (2010) ATM activation by oxidative stress. *Science* 330(6003):517–521.
38. Lowndes NF, Toh GW-L (2005) DNA repair: The importance of phosphorylating histone H2AX. *Curr Biol* 15(3):R99–R102.
39. Revet I, et al. (2011) Functional relevance of the histone gammaH2Ax in the response to DNA damaging agents. *Proc Natl Acad Sci USA* 108(21):8663–8667.
40. de Feraudy S, Revet I, Bezrookove V, Feeney L, Cleaver JE (2010) A minority of foci or pan-nuclear apoptotic staining of gammaH2AX in the S phase after UV damage contain DNA double-strand breaks. *Proc Natl Acad Sci USA* 107(15):6870–6875.
41. Hoffmann S, Spitkovsky D, Radicella JP, Epe B, Wiesner RJ (2004) Reactive oxygen species derived from the mitochondrial respiratory chain are not responsible for the basal levels of oxidative base modifications observed in nuclear DNA of mammalian cells. *Free Radic Biol Med* 36(6):765–773.
42. Kuraoka I, et al. (2000) Removal of oxygen free-radical-induced 5′,8-purine cyclodeoxynucleosides from DNA by the nucleotide excision-repair pathway in human cells. *Proc Natl Acad Sci USA* 97(8):3832–3837.
43. Brooks PJ (2007) The case for 8,5′-cyclopurine-2′-deoxynucleosides as endogenous DNA lesions that cause neurodegeneration in xeroderma pigmentosum. *Neuroscience* 145(4):1407–1417.
44. Citterio E, et al. (1998) Biochemical and biological characterization of wild-type and ATPase-deficient Cockayne syndrome B repair protein. *J Biol Chem* 273(19):11844–11851.
45. Van Raamsdonk CD, et al. (2009) Frequent somatic mutations of GNAQ in uveal melanoma and blue naevi. *Nature* 457(7229):599–602.